Electronic properties of pyroxenes $NaCrSi_2O_6$ and $NaFeSi_2O_6$

S. V. Streltsov,[1,2,*] J. McLeod,[3] A. Moewes,[3] G. J. Redhammer,[4] and E. Z. Kurmaev[1]
[1]*Institute of Metal Physics, S. Kovalevskoy Street 18, 620041 Ekaterinburg GSP-170, Russia*
[2]*Ural State Technical University, Mira Street 19, 620002 Ekaterinburg, Russia*
[3]*Department of Physics and Engineering Physics, University of Saskatchewan, 116 Science Place Saskatoon, Saskatchewan, Canada S7N 5E2*
[4]*Department of Material Science, Division of Mineralogy, University of Salzburg, Hellbrunnerstr. 34, Salzburg A-5020, Austria*
(Received 1 September 2009; revised manuscript received 23 December 2009; published 19 January 2010)

Two pyroxenes, $NaCrSi_2O_6$ and $NaFeSi_2O_6$, are studied with soft x-ray spectroscopy measurements and first principles band structure calculations. The results of O K_a and Si $L_{2,3}$ x-ray emission spectroscopy (XES), and O 1*s* and Si 2*p* x-ray absorption spectroscopy (XAS) measurements are presented. Using a combination of the XAS and XES techniques, the band gaps for these two materials were measured. By comparing the experimental spectra to the results of the band structure calculations in different approximations, we show that pyroxenes should be considered as strongly correlated compounds.

DOI: 10.1103/PhysRevB.81.045118 PACS number(s): 71.27.+a, 78.70.Dm, 78.70.En

I. INTRODUCTION

The unusually rich physical properties of pyroxenes make these compounds, some of which are natural minerals, a very attractive topic of study. Over the last few years pyroxenes have been studied as model low-dimensional systems,[1–4] some of them were found to be ferromagnetic insulators,[5] and others seem to show a fascinating Orbital-Peierls transition.[6] Finally, multiferroic behavior has been recently measured in $(Li,Na)FeSi_2O_6$.[7]

Most of the investigations have been concentrated on the structural and magnetic properties of the pyroxenes, and consequently the electronic structure of pyroxenes has remained obscure. To the best our knowledge, there has not yet been a study using neither optical nor x-ray techniques on the pyroxenes of the $(Li,Na)TM(Si,Ge)_2O_6$ series, where TM is a transition metal ion. Moreover, even the band gaps for these pyroxenes are unknown. An investigation of the electronic properties of pyroxenes is very important not only because of their multiferroic properties, but because in general their magnetic structure is strongly dependent on the actual orbital filling.[8] Moreover depending on the strength of the on-site Hubbard repulsion there can be a qualitatively different description of magnetic properties of some of the pyroxenes. For instance, $NaTiSi_2O_6$ can be considered as a spin-dimer compound[9] or as a net of Haldane chains.[10]

Herein we present a detailed study of the electronic structure of two pyroxenes $NaCrSi_2O_6$ and $NaFeSi_2O_6$ using both experimental x-ray techniques and theoretical band structure calculations. This investigation is important not only for the given materials, but also for all compounds of the $(Li,Na)TM(Si,Ge)_2O_6$ series, since it allows a study of the strength of the electronic correlations, hybridization effects between different ions, and evolution of different spectral characteristics in pyroxenes.

As mentioned above, the electronic structure for $NaCrSi_2O_6$ and $NaFeSi_2O_6$ have not been experimentally investigated before. The valence of the transition metal ions is 3+ in both systems, which corresponds to the formal occupation numbers d^3 for Cr^{3+}, and d^5 for Fe^{3+}. According to the magnetic measurements $NaCrSi_2O_6$ is an antiferromagnetic with $T_N=3$ K,[5] while $NaFeSi_2O_6$ becomes both antiferromagnetically ordered and ferroelectric below 6 K.[7] Herein we not only estimate the band gaps and some other spectral characteristics, but also show the importance of including an on-site Coulomb repulsion in the correct description of electronic properties of pyroxenes.

II. MATERIALS AND METHODS

$NaCrSi_2O_6$ and $NaFeSi_2O_6$ samples were prepared by use of the flux growth method from Na_2CO_3, Cr_2O_3 or Fe_2O_3 and SiO_2 in the exact stoichiometry of the compounds. The starting chemicals were intimately ground together under alcohol and mixed with Na_2MoO_4—acting as the high-temperature solution—in a ratio nutrient to flux=1:10. The syntheses batches (~25 g each) were placed in platinum crucibles, covered with a lid, heated to 1373 K at ambient conditions, and held at this temperature for a period of 48 h. Afterwards the samples were slowly cooled to 873 K at a rate of 0.5 K per hour. The flux could easily be removed in hot water and single crystal clinopyroxene yields were obtained. After removing small amounts of impurity phases (hematite Fe_2O_3, glass, or Cr_2O_3) by hand picking, phase-pure samples were available.

The soft x-ray spectra were measured at beamline 8.0.1 at the advanced light source (ALS) at the Lawrence Berkeley National Laboratory.[11] The $NaCrSi_2O_6$ and $NaFeSi_2O_6$ powder samples were pressed into clean indium foil and mounted in the vacuum chamber. The O 1*s* x-ray absorption spectroscopy (XAS) spectra were measured in the total fluorescence yield (TFY) mode, which provides more bulk sensitivity than electron yield methods. All XAS spectra were normalized to the incident photon current using a highly transparent gold mesh in front of the sample to measure the intensity fluctuations in the photon beam. The XES endstation uses a Rowland circle geometry x-ray spectrometer with spherical gratings and an area sensitive multichannel detector. The instrumental resolving power $(E/\Delta E)$ was approximately 10^3 for the x-ray emission spectroscopy (XES) measurements

and approximately 5×10^3 for the XAS measurements.

The crystallographic data used in the band calculations were taken from Ref. 12 and 13. We utilized the full potential linear augmented plane wave (LAPW)[14] method with either the generalized gradient approximation (GGA) and generalized gradient approximation taking into account on-site Coulomb repulsion with the mean-field method (GGA+U). The exchange correlation potential as proposed by Perdew, Burke and Enzerhof[15] was chosen. The values of on-site Coulomb interaction (U) and Hund's rule coupling (J_H) parameters were taken to be the same as in previous pseudopotential and linear muffin-tin orbitals (LMTO) calculations:[8] U_{Cr} =3.7 eV, U_{Fe}=4.5 eV; J_H=0.8 eV for Cr and J_H=1 eV for Fe. The atomic sphere radii were set as following: R_{Na}=2.2, R_O=1.5 a.u., R_{Si}=1.5 a.u., and R_{Cr}=R_{Fe}=1.9 a.u. The Brillouin-zone (BZ) integration in the course of the self-consistency iterations was performed over a mesh of 100 **k**-points. The parameter of the plane wave expansion was chosen to be $R_{MT}K_{max}$=7, where R_{MT} is the smallest atomic sphere radii and K_{max} - plane wave cutoff.

The difference in the band gaps obtained via LMTO and LAPW calculations are related with the different ways of describing wave functions and applying a U correction in each of these methods. It is well known that in the full-potential LAPW calculations U should smaller than that in LMTO calculations. The typical example is cobaltates.[16,17] Since U and J_H were taken to be the same as in Ref. 8 the band gap in the present study was obtained for Mott-Hubbard system $NaCrSi_2O_6$ to be larger than in Ref. 8. This is in contrast to $NaFeSi_2O_6$ for which LAPW and LMTO give exactly the same values, since the band gap is defined by charge-transfer energy for this compound.

III. ANALYSIS OF XAS AND XES RESULTS

In Figs. 1 and 2 we present the XAS and XES measurements for $NaCrSi_2O_6$ and $NaFeSi_2O_6$. It was recently shown that a combination of these methods can be used to determine the band gap and charge transfer energy values.[18] Energy calibration of the XAS and XES data was performed by comparing the recorded spectra to a subsequently recorded spectrum of a known reference sample. The band gaps were estimated from the experimental spectra by taking the peaks in the second derivatives.

For $NaCrSi_2O_6$ experimental band gap is 4.8 eV. In the GGA calculation the top of the valence band is formed by completely filled $t_{2g}^{\uparrow}$ and the bottom of the conduction band by empty $e_g^{\uparrow}$ states as one can see from Fig. 3. Since the exchange splitting is very large for $NaCrSi_2O_6$ ($\sim$3 eV), the band gap in GGA is defined by the $t_{2g}-e_g$ crystal-field splitting and dispersion of these bands. The band gap in the GGA calculation is 2 eV, this is significantly smaller than the experimental estimate.

The result from a regular GGA calculation can be remarkably improved by accounting for the on-site Coulomb repulsion in the calculation scheme with an additional potential U. Adding this potential results in the additional shift of occupied (downward) and unoccupied (upward) states. In GGA +U the band gap with U_{Cr}=3.7 eV is 3.7 eV, which is closer

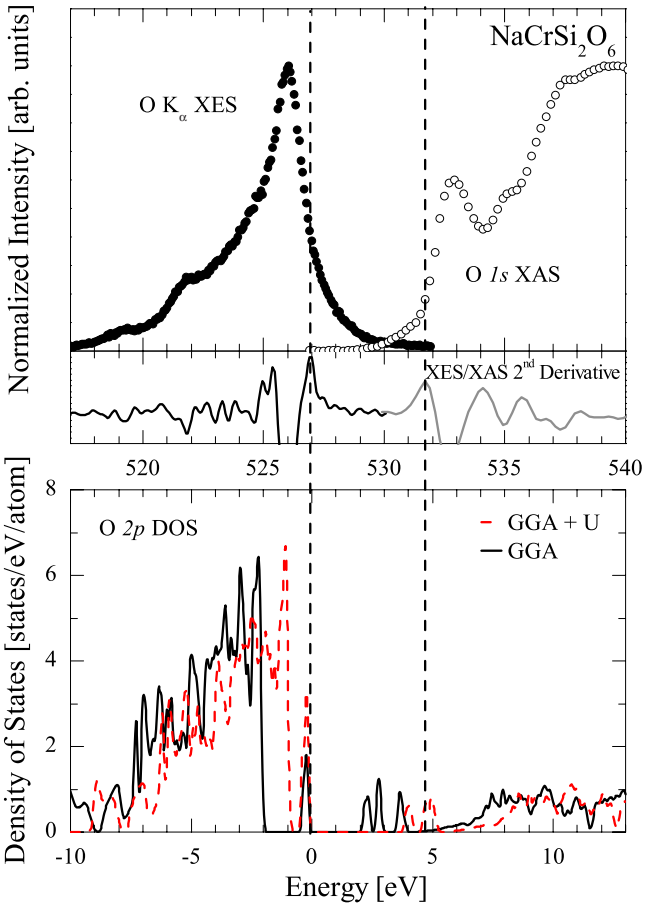

FIG. 1. (Color online) Comparison of the experimental O K_α XES and O 1s XAS spectra (top) with the theoretical O-2p density of states (bottom), obtained by GGA with (red line) and without (black line) including the on-site Coulomb repulsion U, for $NaCrSi_2O_6$. The Fermi energy is at zero.

to the experimental value. The band gap develops between occupied and unoccupied Cr-3d states, which is clearly seen from the DOS plot for closely-related compound $NaCrGe_2O_6$ presented in Fig. 8 of Ref. 8. Thus Cr based pyroxenes may be considered as Mott-Hubbard materials taking into account a non-negligible mixing of O-2p states to the top of the valence band.

In addition to a more plausible value of the band gap, the structure of the density of O-2p states in the GGA+U is closer to the experimental XES spectra. One may see that the GGA+U density of states (DOS) peaks exactly at the same place as experimental spectra, at ~-1 eV (if the Fermi level is set to zero), while GGA results in the peak at ~-2 eV. These peaks correspond to bonding-nonbonding O-2p-Si-3p states. The agreement between the structure of the unoccupied DOS and the experimental O-1s XAS spectra is also better in the GGA+U. The large feature at energies higher than $\sim$8 eV is due to antibonding O-2p-Si-3p states, while the lower energy structure at $\sim$4–8 eV is related to the substantial hybridization between the unoccupied transition metal -3d and the O-2p states.

The general structure of O K_α XES and O-1s XAS spectra for $NaFeSi_2O_6$ presented in Fig. 2 is similar to that of

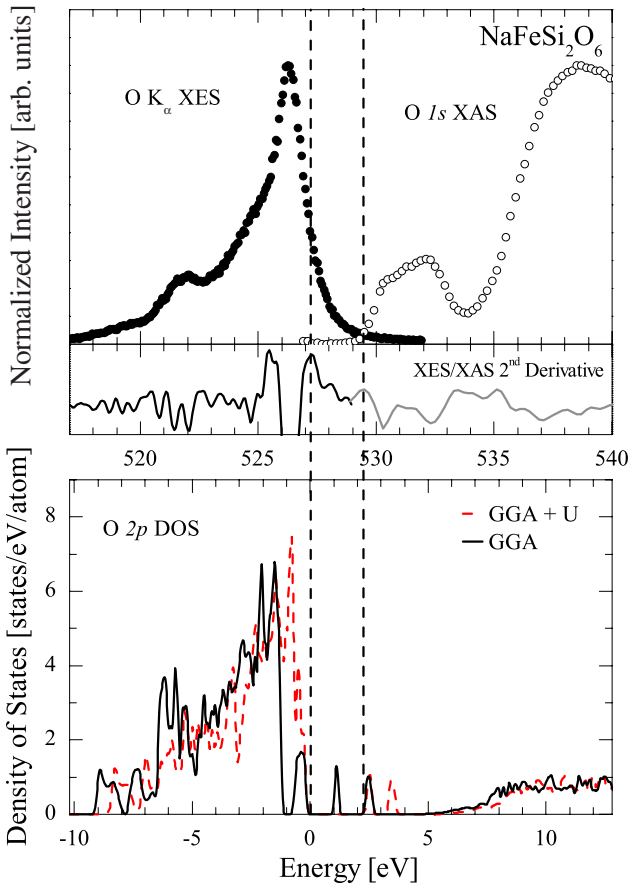

FIG. 2. (Color online) Comparison of the experimental O K_α XES and O 1s XAS spectra (top) with the theoretical O-2p density of states (bottom), obtained by GGA with (red line) and without (black line) including the on-site Coulomb repulsion U, for $NaFeSi_2O_6$. The Fermi energy is at zero.

$NaCrSi_2O_6$. However one may notice that both the experimental and theoretical band gaps are smaller than those obtained for $NaCrSi_2O_6$, while the on-site Coulomb repulsion parameter U is larger for Fe. Similar changes in the band gap

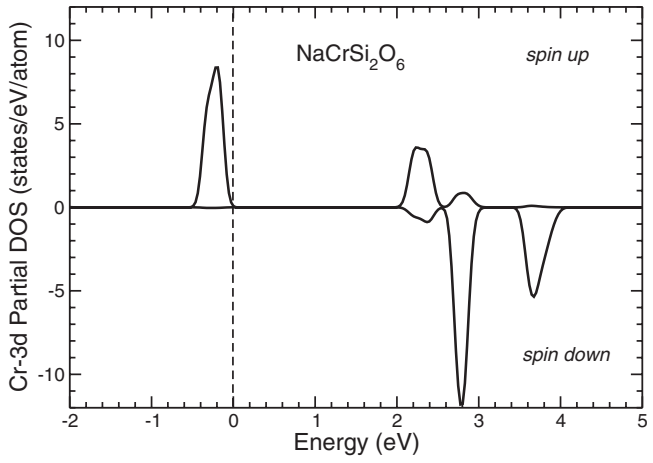

FIG. 3. Cr-3d DOS obtained by GGA. Positive (negative) values of DOS correspond to spin up (spin down). The Fermi energy is at zero.

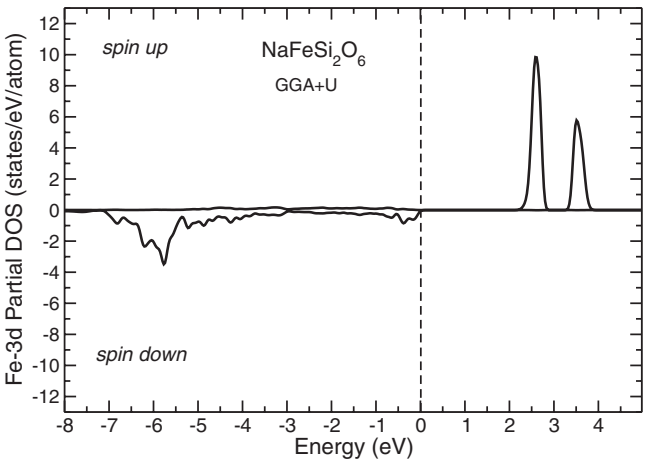

FIG. 4. Fe-3d DOS obtained by GGA+U. Positive (negative) values of DOS correspond to spin up (spin down). The Fermi energy is at zero.

values as seen in the pyroxenes going from Fe to Cr were observed in perovskite materials.[19] The reduction of the band gap occurs due to transition to a charge-transfer regime in $NaFeSi_2O_6$.

The lower Hubbard band is clearly seen in the lower panel Fig. 1 just below the Fermi level for the $NaCrSi_2O_6$ (one may also consult Fig. 8 from Ref. 8, where DOS for similar compound $NaCrGe_2O_6$ is presented). In contrast For $NaFeSi_2O_6$ the top of the valence band is defined by O-2p states, while the occupied Fe-3d states are located deeper in energy (see Fig. 4).

One may note that the actual change of the U-parameter going from Cr to Fe based pyroxenes in the calculations is not that large (0.8 eV), while the effect is quite pronounced. This can be explained in the following way: since Fe^{3+} has fully occupied one spin subshell the effective Coulomb repulsion for this configuration significantly increases due to Hund's exchange J_H and equals to: $U_{eff}^{Fe^{3+}} = U^{Fe^{3+}} + 4J_H$, while for Cr^{3+}:$U_{eff}^{Cr^{3+}} = U^{Cr^{3+}} - J_H$. One may calculate U_{eff} using a standard definition,

$$U_{eff} = E(d^{n+1}) + E(d^{n-1}) - 2E(d^n), \quad (1)$$

(where E is the total energy of the given configuration) and taking explicitly the number of J_H each configuration into account.

Both the basic growth of the U parameter due to the increase in the number of electrons and accounting for the different number of the Hund's rule exchanges J_H leads to a significant shift of the lower Hubbard band to the lower energies in $NaFeSi_2O_6$. In addition the charge-transfer energy Δ is known to decrease with increase in the number of electrons in 3d shell of transition metal ion.[20,21] If for Cr^{3+} $\Delta \sim 5.2$ eV,[21] then for Fe^{3+} it is $\Delta \sim 2.5-3.5$ eV (depending on the system and type of estimation).[20] Thus the band gap in $NaFeSi_2O_6$ is defined not by the effective Coulomb repulsion as in $NaCrSi_2O_6$, but by the significantly smaller charge-transfer energy Δ. The theoretical estimation of the band gap within the GGA+U approach for $NaFeSi_2O_6$ is 2.3 eV,

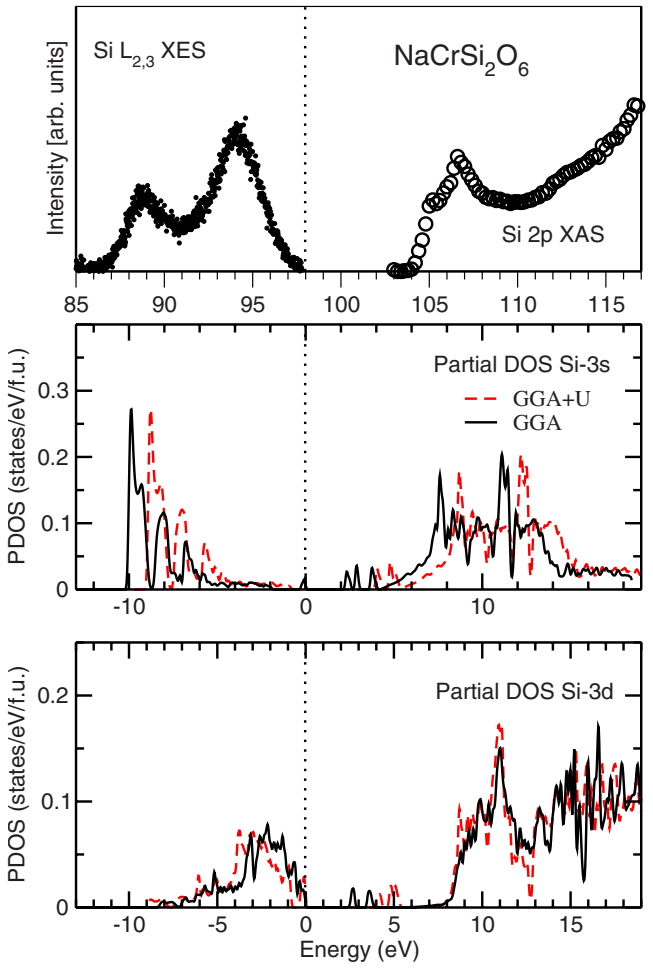

FIG. 5. (Color online) Comparison of experimental Si $L_{2,3}$ XES and Si-2*p* XAS spectra (top) with theoretical Si-3*s* (middle) and Si-3*d* (bottom) density of states, obtained by GGA with (red line) and without (black line) account of on-site Coulomb repulsion *U*, for $NaCrSi_2O_6$. The Fermi energy is at zero.

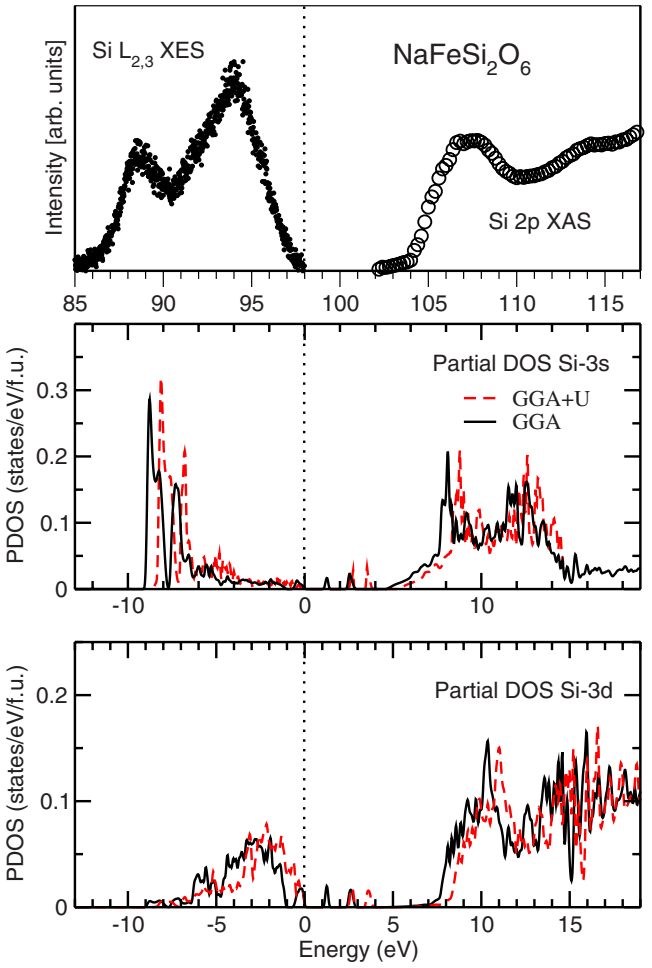

FIG. 6. (Color online) Comparison of experimental Si $L_{2,3}$ XES and Si-2*p* XAS spectra (top) with theoretical Si-3*s* (middle) and Si-3*d* (bottom) density of states, obtained by GGA with (red line) and without (black line) account of on-site Coulomb repulsion *U*, for $NaFeSi_2O_6$. The Fermi energy is at zero.

which is closed to experimentally measured value of 2.2 eV. The GGA again underestimates the value of the band gap giving E_g=0.9 eV.

The low energy structure of O-1*s* XAS spectra is also different in $NaCrSi_2O_6$ and $NaFeSi_2O_6$. This should be related with a different number of unoccupied states in the TM-3*d* shell (there are 3 t_{2g} and 4 split by exchange interaction e_g states in the case of Cr^{3+} and only 3 t_{2g} and 2 e_g states for Fe^{3+}), but this is not clearly seen in direct comparison of the GGA+U O-2*p* partial DOS with experimental spectra. The discrepancies can be connected with core-hole effects, which has been shown to shift the O-2*p* unoccupied states closer to the onset of the conduction band in metal oxides.[22]

An additional check of the validity of the GGA or GGA +U electronic structure calculations of pyroxenes can be performed with the help of Si $L_{2,3}$- emission and absorption spectra, which probe Si-3*s*3*d* occupied and vacant states, respectively. The results of Si $L_{2,3}$ XES and Si-2*p* XAS measurements of $NaCrSi_2O_6$ and $NaFeSi_2O_6$ are presented in Figs. 5 and 6. The Si $L_{2,3}$ XES are similar for both compounds and consist of two subbands located at 88.5 and 94.0 eV. According to our calculations the lowest peak is due to Si-3*s* states while one lying higher in energy originates from Si-3*d* states. In the XES spectra the Si-3*s* states are separated from the Si-3*d* states by ~5 eV for $NaCrSi_2O_6$ and by ~5.5 eV for $NaFeSi_2O_6$. The GGA+U and GGA calculations suggest a splitting of ~5 eV and ~8 eV, respectively, for $NaCrSi_2O_6$. Clearly the GGA+U calculation is closer to reproducing the experimental splitting. For $NaFeSi_2O_6$ the GGA+U and GGA calculations suggest a splitting of ~5.5 eV and ~5 eV. Here the difference is rather minor, but the GGA+U calculation is again closer to reproducing the experimental splitting than the GGA calculation. The near-edge structure of Si-2*p* XAS is formed by Si-3*s* and Si-3*d* states. One can see that GGA+U Si unoccupied 3*s*3*d* states are shifted to slightly higher energies as a whole with respect to GGA Si unoccupied 3*s*3*d* states. In particular, the bulk Si-3*s* states which form the main onset of the unoccupied spectrum (and therefore are of greatest importance to the onset of the measured XAS) are on ~1.5 eV and ~1 eV higher in the GGA+U calculation than in the GGA calculation for $NaCrSi_2O_6$ and $NaFeSi_2O_6$, respectively. These

shifts are in better agreement with experimental spectra, especially since the effect of the Si-2*p* core-hole on the measured XAS would serve to shift the XAS to lower energies than predicted by the DOS. Therefore, we can conclude that both the oxygen and silicon x-ray emission and absorption spectra of $NaCrSi_2O_6$ and $NaFeSi_2O_6$ are in good agreement with GGA+U calculations which means that accounting for the on-site electron correlation is necessary for a correct description of the electronic properties of pyroxenes.

IV. SUMMARY

Using combination of x-ray measurements and first principles band structure calculations we show that pyroxenes of $(Li,Na)TM(Si,Ge)_2O_6$ must be considered as strongly correlated materials. Neglect of the on-cite Coulomb interaction in the GGA results in considerable underestimation of the band gap, while explicit account of correlations (U) in the mean-field way by GGA+U significantly improves agreement between theory and experiment.

ACKNOWLEDGMENTS

We are grateful to N. Skorikov for fruitful discussions concerning the present investigation. This work is supported by Dynasty Foundation and International Center for Fundamental Physics in Moscow, by the Russian Ministry of Science and Education via Programs No. 02.740.11.0217 and No. MK-360.2009.2 and together with the Civil Research and Development Foundation through Grant No. Y4-P-05-15, by the Russian Foundation for Basic Research through Grants No. RFFI-10-02-96011 and No. RFFI-10-02-00140, the Natural Sciences and Engineering Research Council of Canada (NSERC), and the Canada Research Chair program.

*streltsov.s@gmail.com

[1] J. L. Gavilano, S. Mushkolaj, H. R. Ott, P. Millet, and F. Mila, Phys. Rev. Lett. **85**, 409 (2000).
[2] P. Millet, F. Mila, F. C. Zhang, M. Mambrini, A. B. Van Oosten, V. A. Pashchenko, A. Sulpice, and A. Stepanov, Phys. Rev. Lett. **83**, 4176 (1999).
[3] B. Pedrini, J. L. Gavilano, H. R. Ott, S. M. Kazakov, J. Karpinski, and S. Wessel, Eur. Phys. J. B **55**, 219 (2007).
[4] M. D. Lumsden, G. E. Granroth, D. Mandrus, S. E. Nagler, J. R. Thompson, J. P. Castellan, and B. D. Gaulin, Phys. Rev. B **62**, R9244 (2000).
[5] A. N. Vasiliev, O. L. Ignatchik, A. N. Sokolov, Z. Hiroi, M. Isobe, and Y. Ueda, Phys. Rev. B **72**, 012412 (2005).
[6] M. J. Konstantinović, J. van den Brink, Z. V. Popović, V. V. Moshchalkov, M. Isobe, and Y. Ueda, Phys. Rev. B **69**, 020409(R) (2004).
[7] S. Jodlauk, P. Becker, J. A. Mydosh, D. I. Khomskii, T. Lorenz, S. V. Streltsov, D. C. Hezel, and L. Bohaty, J. Phys.: Condens. Matter **19**, 432201 (2007).
[8] S. V. Streltsov and D. I. Khomskii, Phys. Rev. B **77**, 064405 (2008).
[9] S. V. Streltsov, O. A. Popova, and D. I. Khomskii, Phys. Rev. Lett. **96**, 249701 (2006).
[10] Z. S. Popović, Z. V. Šlijivančanin, and F. R. Vukajlović, Phys. Rev. Lett. **93**, 036401 (2004).
[11] J. J. Jia, T. A. Callcot, J. Yurkas, A. W. Ellis, F. J. Himpsel, M. G. Samant, J. Stohr, and D. L. Ederer, Rev. Sci. Instrum. **66**, 1394 (1995).
[12] M. Origlieri, R. T. Downs, R. M. Thompson, C. J. S. Pommier, M. B. Denton, and G. E. Harlow, Am. Mineral. **88**, 1025 (2003).
[13] O. Ballet, J. M. D. Coey, G. Fillion, A. Ghose, A. Hewat, and J. R. Regnard, Phys. Chem. Miner. **16**, 672 (1989).
[14] P. Blaha *et al.*, WIEN2k, An Augmented Plane Wave+Local Orbitals Program for Calculating Crystal Properties, Karlheinz Schwarz, Techn. Universität Wien, Austria, 2001.
[15] J. P. Perdew, K. Burke, and M. Ernzerhof, Phys. Rev. Lett. **77**, 3865 (1996).
[16] I. A. Nekrasov, S. V. Streltsov, M. A. Korotin, and V. I. Anisimov, Phys. Rev. B **68**, 235113 (2003).
[17] K. Knížek, Z. Jirák, J. Hejtmánek, P. Novák, and W. Ku, Phys. Rev. B **79**, 014430 (2009).
[18] E. Z. Kurmaev, R. G. Wilks, A. Moewes, L. D. Finkelstein, S. N. Shamin, and J. Kuneš, Phys. Rev. B **77**, 165127 (2008).
[19] T. Arima, Y. Tokura, and J. B. Torrance, Phys. Rev. B **48**, 17006 (1993).
[20] A. E. Bocquet, T. Mizokawa, T. Saitoh, H. Namatame, and A. Fujimori, Phys. Rev. B **46**, 3771 (1992).
[21] A. E. Bocquet, T. Mizokawa, K. Morikawa, A. Fujimori, S. R. Barman, K. Maiti, D. D. Sarma, Y. Tokura, and M. Onoda, Phys. Rev. B **53**, 1161 (1996).
[22] J. A. McLeod, R. G. Wilks, N. A. Skorikov, L. D. Finkelstein, M. Abu-Samak, E. Z. Kurmaev, and A. Moewes, arXiv:0908.1581 (unpublished).